LEVEL II

AD A071342

AN INVESTIGATION OF PORTABLE ELECTROMAGNETIC PULSE SIMULATORS/ALTERNATE SIMULATORS

M. I. Sancer
S. Siegel
A. D. Varvatsis

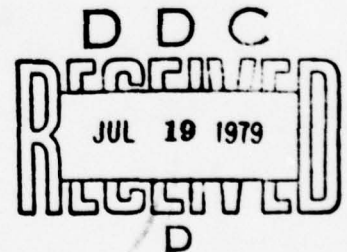TDR, Inc.
Marina del Rey, CA 90291

June 1979

Final Report

Approved for public release; distribution unlimited.

DDC
RECEIVED
JUL 19 1979
D

Prepared for
Director
DEFENSE NUCLEAR AGENCY
Washington, DC 20305

AIR FORCE WEAPONS LABORATORY
Air Force Systems Command
Kirtland Air Force Base, NM 87117
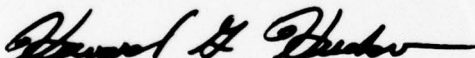
DDC FILE COPY

79 07 17 072

This final report was prepared by TDR, Inc., Marina del Rey, California, under Contract F29601-77-C-0090, Job Order WDNE3206, with the Air Force Weapons Laboratory, Kirtland Air Force Base, New Mexico. Capt H. G. Hudson was the Laboratory Project Officer-in-Charge.

This report has been reviewed by the Office of Information (OI) and is releasable to the National Technical Information Service (NTIS). At NTIS it will be available to the general public, including foreign nationals.

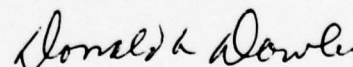This technical report has been reviewed and is approved for publication.

HOWARD G. HUDSON
Capt, USAF
Project Officer

P. PHILIP CASTILLO
Chief, Technology Branch

FOR THE COMMANDER

DONALD A. DOWLER
Col, USAF
Chief, Electromagnetics Division

REPORT DOCUMENTATION PAGE		READ INSTRUCTIONS BEFORE COMPLETING FORM
1. REPORT NUMBER AFWL-TR-78-200	2. GOVT ACCESSION NO.	3. RECIPIENT'S CATALOG NUMBER
4. TITLE (and Subtitle) AN INVESTIGATION OF PORTABLE ELECTROMAGNETIC PULSE SIMULATORS/ALTERNATE SIMULATORS.		5. TYPE OF REPORT & PERIOD COVERED Final Report.
		6. PERFORMING ORG. REPORT NUMBER
7. AUTHOR(s) M. I. Sancer S. Siegel A. D. Varvatsis		8. CONTRACT OR GRANT NUMBER(s) F29601-77-C-0090
9. PERFORMING ORGANIZATION NAME AND ADDRESS TDR, Inc., P. O. Box 9695 Marina del Rey, CA 90291		10. PROGRAM ELEMENT, PROJECT, TASK AREA & WORK UNIT NUMBERS 62704H WDNE3206
11. CONTROLLING OFFICE NAME AND ADDRESS Director Defense Nuclear Agency Washington D C 20305		12. REPORT DATE June 1979
		13. NUMBER OF PAGES 48
14. MONITORING AGENCY NAME & ADDRESS(if different from Controlling Office) Air Force Weapons Laboratory (ELTI) Kirtland Air Force Base, NM 87117		15. SECURITY CLASS. (of this report) UNCLASSIFIED
		15a. DECLASSIFICATION/DOWNGRADING SCHEDULE

16. DISTRIBUTION STATEMENT (of this Report)

Approved for public release; distribution unlimited.

17. DISTRIBUTION STATEMENT (of the abstract entered in Block 20, if different from Report)

18. SUPPLEMENTARY NOTES

This research was sponsored by the Defense Nuclear Agency under Subtask
R99QNXEB200, Work Unit 71, Title: Hardness Surveillance.

19. KEY WORDS (Continue on reverse side if necessary and identify by block number)

Electromagnetic Pulse Scattering
Portable/Alternate EMP Simulators
Magnetic Field Integral Equation
Singularity Expansion Method
Path Zoning Method

20. ABSTRACT (Continue on reverse side if necessary and identify by block number)

A theory is developed which defines the technical objectives for portable EMP
simulator experiments and calculations. It is shown that under certain condi-
tions, a configuration of portable sources need only excite a prescribed exter-
nal interaction response on a class of systems. Under these conditions, the
source configuration will excite the same electrical quantities within the
system as would an EMP. Considerable attention is devoted to the demonstration
that these conditions must include an accounting for the external environment

to the system under test as well as the degree of electromagnetic rigidity of the portable sources. Finally, calculations that were chosen to address the plausibility of achieving the described external interaction objectives are presented and interpreted according to the required conditions.

Accession For		
NTIS GRA&I	✗	
DDC TAB		
Unannounced		
Justification		
By		
Distribution/		
Availability Codes		
Dist	Avail and/or special	
A		

PREFACE

Part of the theory presented in this report was developed while one of the authors, Maurice Sancer, was consulting for R & D Associates.

CONTENTS

3

ILLUSTRATIONS

SECTION I

INTRODUCTION

The broad objective of this effort is to guide the experimental invesitgation of electromagnetic pulse (EMP) simulation by portable simulators. We perform two distinctly different types of analysis directed toward this objective. First, we develop a theory that results in the definition of technical objectives for both experiments and calculations. Finally, we perform calculations to determine whether a very idealized experiment could possibly achieve the required objectives.

The analysis resulting in the technical objectives consists of developing the form of a transfer operator equation in sufficient detail to identify the significance of all terms. Specifically, attention is directed toward clearly identifying the physical quantities related by the transfer operator as well as the physical quantities on which the transfer operator depends. To facilitate the discussion of the physical quantities it is necessary to discuss the type of system we wish to excite with the portable simulators. The class of systems for which this study is applicable are those systems that are, in effect, imperfectly sealed metallic enclosures. Important systems that belong to this class are aircraft, missiles, ships, and tanks. The breaks in these enclosures are referred to as apertures and they might correspond to windows, hatches, or portions of deliberate antennas that are intended to allow energy to flow into the system.

The operator equation relates electrical quantities excited within the actual enclosure (system) to the current density induced on metallic seals placed over all of the apertures of the imperfectly sealed enclosure. The existence of this equation would seem to imply that if a configuration of portable sources excited the same current density on the

5

seals as did an EMP, then internal electrical quantities within the enclosure of the unsealed system would be identically excited by either the EMP or the portable source configuration. This would be the case under the following conditions; the portable sources must be electromagnetically rigid, i.e., unaffected by the presence of any scatterer, and the external environment of the system must be the same for the portable source configuration as for the EMP. For example, an aircraft having the appropriate seals correctly excited by rigid portable sources when parked on the ground, can only be viewed as having been excited by the corresponding EMP when it is still resting on the ground and in particular is not in free flight.

Even with these limitations, we see that it is possible to assist the alternate simulation program by performing only external interaction measurements or calculations. The initial source configuration can be determined by employing only external interaction considerations. We emphasize that we expect the focus to be on external interaction only in the initial program stages because we anticipate that the local sources will not be capable of exciting exactly the same external interaction quantities on the metallic seals as would an EMP. In order to assess these effects as well as non-rigidity degradation, we expect that internal electrical quantities will have to be measured for excitation by the portable source configuration as well as for excitation by a more orthodox simulator which represents the EMP excitation.

The environment and source rigidity conditions previously discussed result from the dependence of the transfer operator on these factors and not the quantities this operator relates. This source rigidity requirement causes special concern in that any physically realizable portable source is going to

have structure that can interact with the fields reflected
from the system under test. This is of particular concern
because it is presently anticipated that the configuration
of portable sources will be in close proximity to the system
under test. The choice of calculations to perform, which
represented an idealized experiment, was made with the issue
of source rigidity being a distinct factor.

The problem for which we made our calculations was the
excitation of a sphere in free space by a plane wave and by
various configurations of idealized local sources. These
calculations were performed in the frequency domain for a
range of frequencies starting at zero and extending to approx-
imately three times the first resonant frequency of the sphere.
Well-established plane wave solutions exist for this problem
and our method of obtaining our plane wave solution can be
verified by comparison of our results to the established re-
sults. This is necessary because our method of obtaining the
plane wave solution is the same as our method of obtaining the
source configuration results and no data is presently available
to verify those calculations. As a general conclusion, our
calculations indicate that our choice of local source config-
uration can approximately excite the desired external inter-
action current density at a shorted point of entry only if at
least one local source is in close proximity to the shorting
surface. This result increases the need to study the effect
of the degree of rigidity of physically realizable sources on
the alternate simulation problem.

SECTION II

THEORETICAL BACKGROUND

This investigation concerns the local excitation of systems that are predominantly metallic and is valid for those frequencies or times for which the metal can be considered to be perfectly conducting. The equations that form the basis of this investigation of portable EMP simulators is a set of equations that recognizes those essential features of classical aperture coupling analysis that have relevance to complex systems. Since this approach is based on aperture coupling equations, one might be concerned with its relevance to other types of penetrators, e.g., deliberate antennas. Such penetrators have associated apertures or else no energy could penetrate the sealed skin of the system corresponding to that penetrator.

First we will present the general form of the equations that provide the basis of this study and draw all of our theoretical conclusions by referring to properties of this general form. Next we will present a somewhat detailed derivation of these general equations for a complex interaction situation in order to give a more concrete meaning to the general properties on which we based our theoretical conclusions. The form of the underlying equation is as follows

$$L \underline{J}_m(\underline{r}') = \underline{J}_{E.I.}(\underline{r}) \tag{1}$$

where the meaning and significance of each term requires considerable attention. First, we emphasize that equation 1 describes the relationship between electrical quantities on two different physical systems. One system is the actual system of interest and the other system is that original system modified by metallic shorting surfaces covering all apertures (including those associated with antennas). For illustrative purposes

8

consider the system depicted in figure 1. One system is the aircraft in its environment with the apertures S_1 and S_2 unmodified and the other system needed to give equation 1 meaning is the same aircraft in the same environment with metallic seals covering S_1 and S_2. In equation 1, the notation $\underline{J}_m$ was chosen to denote "magnetic current," but it is simply $\hat{n}(\underline{r}') \times \underline{E}_t(\underline{r}')$ where $\underline{r}'$ varies over all of the mathematical surfaces corresponding to the open apertures in the original system, $\hat{n}(\underline{r}')$ is the outward normal at $\underline{r}'$, and $\underline{E}_t(\underline{r}')$ is the tangential component of the electric field induced in the open aperture. The quantity $\underline{J}_{E.I.}(\underline{r})$ is the "external interaction" current density induced on the shorted system with $\underline{r}$ ranging only over the shorting surfaces. It is important to note that even though $\underline{r}$ and $\underline{r}'$ refer to different physical systems, they mathematically refer to the same set of points. This distinction allows a discussion of the mathematical nature of equation 1 that is not confused by the dual physical nature of the problem. It remains to discuss the meaning of L in equation 1 to proceed. More specifically, L is a linear operator that depends on a variety of quantities associated with the system, its environment and certain aspects of its excitation. Just what these quantities are plays an essential role in the underlying theory of portable EMP simulators and we will elaborate on what these quantities are when presenting the details for the system depicted in figure 1.

It is now necessary to introduce an additional equation to augment the information contained in equation 1. This equation also represents a general form and is

$$Q_\beta = L_\beta \underline{J}_m(\underline{r}') \tag{2}$$

This equation is a mathematical statement of the fact that $\underline{J}_m(\underline{r}')$ is sufficient to determine a variety of electrical

9
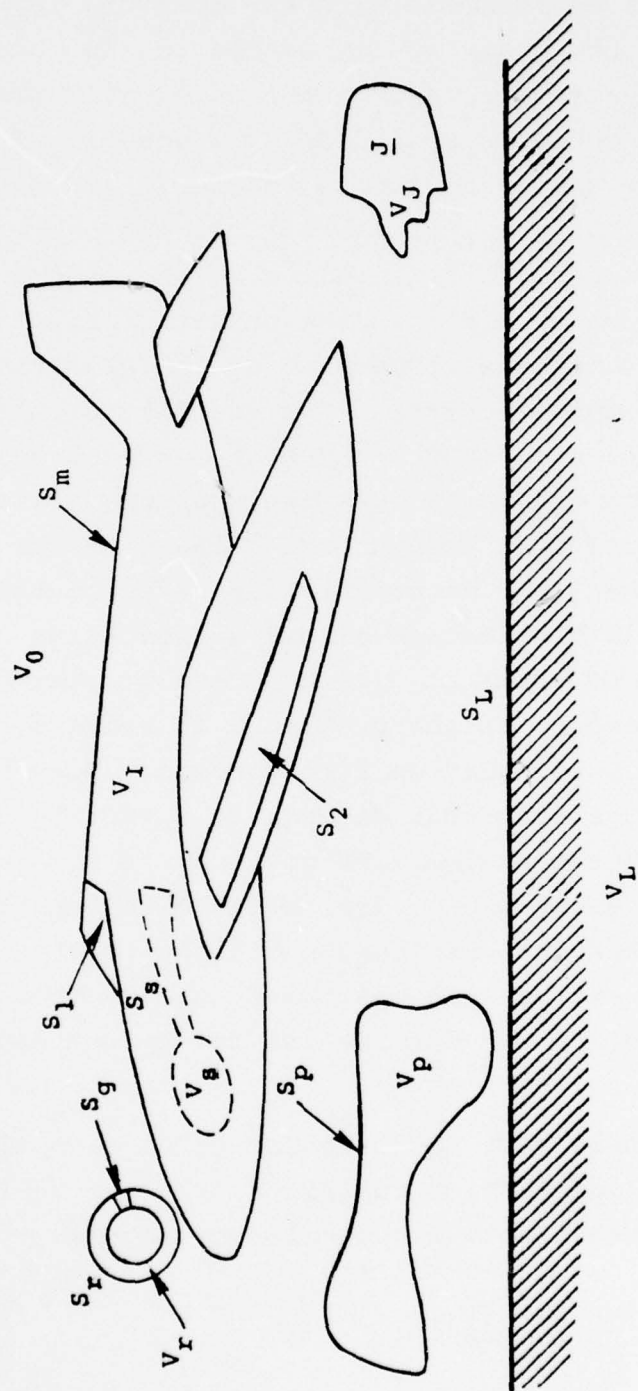
Figure 1. Aircraft and its Environment with Rigid and Non-Rigid Sources

Q_β (e.g., β can correspond to a voltage, a current, or a field component) that are excited within the system by fields penetrating through the apertures. In equation 2, L_β is a linear operator that depends on the internal structure of the system and the choice of the internal electrical quantity that is being determined. Next we introduce a step, the legitimacy of which is currently being studied using a field equivalence point of view. Specifically, it is assumed that the L appearing in equation 1 has a unique inverse, L^{-1}, so that from equation 1 we can obtain

$$\underline{J}_m = L^{-1} \underline{J}_{E.I.} \tag{3}$$

Combining equations 2 and 3 we obtain

$$Q_\beta = T_\beta^\alpha \underline{J}_{E.I.} \tag{4}$$

where

$$T_\beta^\alpha = L_\beta L^{-1} \tag{5}$$

and the superscript α is explicity introduced to indicate that T_β^α depends on the environment external to the system. If the same system were placed in two different environments, then the α designation for each environment could change to accommodate a mathematical representation of the fact that

$$T_\beta^{\alpha_1} \neq T_\beta^{\alpha_2} \tag{6}$$

if the external environments for the same system are sufficiently different. Part of what we shall mean by the external environment is the physical structure of the portable EMP simulators that are being investigated. When we discuss the details

11

with the system and environment depicted in figure 1, we shall emphasize this source structure dependence and make a crucial distinction between rigid and nonrigid sources.

It is possible to present all of the portable simulator theory on equation 4; however, that equation will be modified to conform to the prevalent notion that both the external interaction current density $\underline{J}_{E.I.}$ and the external interaction charge density $\sigma_{E.I.}$ are required for the ultimate determination of the internal quantities Q_β. For non-zero frequency, it follows from $\nabla_s \cdot \underline{J}_{E.I.} = i\omega\sigma_{E.I.}$ that $\underline{J}_{E.I.}$ suffices to determine $\sigma_{E.I.}$, so the requirement that $\sigma_{E.I.}$ be separately determined must be superfluous. There are a number of possibilities why it might be convenient to separately view $\sigma_{E.I.}$ as a desired input and viewing it as such leads to the following decomposition of equation 4

$$Q_\beta = T^\alpha_{J\beta}\underline{J}_{E.I.} + T^\alpha_{\sigma\beta}\sigma_{E.I.} \tag{7}$$

as the basic equation.

At this point we could present the underlying theory of portable EMP simulators by referring to either equation 4 or equation 7 if we did not have to deal with the real physical structure of the portable sources.

The means whereby this aspect enters the consideration is rather complex and is treated by giving a more explicit meaning to these equations. Specifically, this will be accomplished by deriving more explicit representations for equation 1 and equation 2 for the situation depicted in figure 1. First we introduce the following definitions:

S_m: the surface of the metallic enclosure (aircraft) augmented by the mathematical surfaces S_1 and S_2

V_L: is the volume of a lossy medium in the proximity of the enclosure (earth, water)

12

S_L: the surface bounding V_L

V_p: the volume of an object in the proximity of the enclosure (i.e., an aircraft carrier)

S_p: the surface bounding V_p

V_s: the volume of a subsystem contained within the enclosure

S_s: the surface bounding V_s

V_0: the volume exterior to S_m bounded by S_m, S_p, S_L, S_r, and the hemisphere at infinity

V_I: the volume interior to S_m bounded by S_m and S_s

V_J: the volume of a rigid source of an electromagnetic wave, $\underline{J}$, and it is contained in V_0

V_r: the volume of the portable radiator

S_r: the surface of the portable radiator

S_g: the portion of S_r over which the surface tangential electric field is rigidly specified

The essential equation that this approach is based on is the dyadic identity

$$\int_V \left\{ \underline{A}(\underline{r}') \cdot \left[\nabla' \times \nabla' \times \underline{\underline{D}}(\underline{r}';\underline{r}) \right] - \left[\nabla' \times \nabla' \times \underline{A}(\underline{r}') \right] \cdot \underline{\underline{D}}(\underline{r}';\underline{r}) \right\} dV'$$

$$= \int_S \left\{ \underline{A}(r') \cdot \left[\hat{n}(\underline{r}') \times \left\{ \nabla' \times \underline{\underline{D}}(\underline{r}';\underline{r}) \right\} \right] + \left[\left(\nabla' \times \underline{A}(\underline{r}') \right) \times \hat{n}(\underline{r}') \right] \cdot \underline{\underline{D}}(\underline{r}';\underline{r}) \right\} dS' \tag{8}$$

where $\underline{A}(\underline{r}')$ and $\underline{\underline{D}}(\underline{r}';\underline{r})$ are, at this point, a general vector and a general dyadic that must satisfy certain behavior requirements (e.g., differentiability) but not necessarily any equations. In equation 8, S is the surface bounding V and $\hat{n}(\underline{r}')$ is the outward normal to V. Next, the volume, bounding surface, $\underline{A}(\underline{r}')$, and $\underline{\underline{D}}(\underline{r}';\underline{r})$ are specialized. V is chosen, in turn, as V_0 and V_I and $\underline{A}(\underline{r}')$ is chosen as $\underline{H}_0(\underline{r}')$ and $\underline{H}_i(\underline{r}')$. We also choose $\underline{\underline{D}}(\underline{r}';\underline{r})$ as appropriate Green's

13

dyadics $\left(\underline{\underline{G}}_0(\underline{r}';\underline{r}),\underline{\underline{G}}_I(\underline{r}';\underline{r})\right)$ that satisfy the vector wave equation

$$\left(\nabla'\times\nabla'\times-k_0^2\right)\underline{\underline{G}}_\alpha(\underline{r}_\alpha',\underline{r}_\alpha) = \underline{\underline{I}}\delta(\underline{r}_\alpha'-\underline{r}_\alpha) \quad \alpha=0,I \quad \underline{r}_\alpha',\underline{r}_\alpha\epsilon V_\alpha \quad (9)$$

and subsequently the α subscript of $\underline{r}$ and $\underline{r}'$ will automatically be implied by the subscript on $\underline{\underline{G}}_\alpha$ when it is not explicitly indicated. Boundary conditions to be satisfied are

$$\hat{n}(\underline{r}')\times\left(\nabla'\times\underline{\underline{G}}_I(\underline{r}',\underline{r})\right) = 0 \quad \underline{r}'\epsilon S_m \tag{10}$$

$$\hat{n}(\underline{r}')\times\left(\nabla'\times\underline{\underline{G}}_0(\underline{r}',\underline{r})\right) = 0 \quad \underline{r}'\epsilon S_r US_p US_m \tag{11}$$

$$\hat{n}(\underline{r}')\times\left(\nabla'\times\underline{\underline{G}}_0(\underline{r}',\underline{r})\right) = \hat{n}(\underline{r}')\times\left(\nabla'\times\underline{\underline{G}}_L(\underline{r}',\underline{r})\right) \quad r'\epsilon S_L \tag{12a}$$

$$\hat{n}(\underline{r}')\times\epsilon_0\underline{\underline{G}}_0(\underline{r}',\underline{r}) = \hat{n}(\underline{r}')\times\epsilon\underline{\underline{G}}_L(\underline{r}',\underline{r}) \quad \underline{r}'\epsilon S_L \tag{12b}$$

The equation satisfied by $\underline{\underline{G}}_L(\underline{r}',\underline{r})$ is

$$\left(\nabla'\times\nabla'\times-\omega^2\mu_0\epsilon\right)\underline{\underline{G}}_L(\underline{r}',\underline{r}) = 0 \quad \underline{r}'\epsilon V_L,\underline{r}\epsilon V_0 \tag{13}$$

The equations satisfied by the $H_\alpha(\underline{r}')$ are

$$\left(\nabla'\times\nabla'\times-k_0^2\right)\underline{H}_\alpha(\underline{r}') = \begin{cases} 0 & \alpha=I \\ \nabla'\times\underline{J}(\underline{r}') & \alpha=0 \end{cases} \tag{14}$$

It also follows from Maxwell's equations

$$\nabla'\times\underline{H}_\alpha(\underline{r}') = -i\omega\epsilon_0\underline{E}_\alpha(\underline{r}') \quad \underline{r}'\epsilon S_m \tag{15}$$

Substituting equations 9, 14, and 15 into 8 for $V=V_0$ or V_I and using the property of the δ function, we obtain

14

$$\underline{H}_0(\underline{r}_0) = \underline{I}(\underline{r}_0) + \sum_{q=m,p,r,L} \int_{S_q} \left\{ \hat{n}_{q'}, \underline{E}_0, \underline{H}_0, \underline{\underline{G}}_0 \right\} dS'$$

$$+ \int_{S_\infty} \left\{ \hat{a}_{r''}, \underline{E}_0, \underline{H}_0, \underline{\underline{G}}_0 \right\} dS' \tag{16}$$

$$\underline{H}_I(\underline{r}_I) = \sum_{q=m,s} \int_{S_q} \left\{ \hat{n}_{q'}, \underline{E}_I, \underline{H}_I, \underline{\underline{G}}_I \right\} dS' \tag{17}$$

where $\hat{a}_{r'}$ is the unit outward normal to the sphere at infinity S_∞,

$$\int_S \left\{ \hat{n}, \underline{E}, \underline{H}, \underline{\underline{G}} \right\} dS'$$

$$\equiv \int_S \left\{ \underline{H}(\underline{r}') \cdot \left[\hat{n}(\underline{r}') \times \left\{ \nabla' \times \underline{\underline{G}}(\underline{r}';\underline{r}) \right\} \right] + i\omega\epsilon \left[\hat{n}(\underline{r}') \times \underline{E}(\underline{r}') \right] \cdot \underline{\underline{G}}(\underline{r}';\underline{r}) \right\} dS' \tag{18}$$

where ϵ is the appropriate dielectric permittivity and

$$\underline{I}(\underline{r}_0) = \int_{V_J} \nabla' \times \underline{J}(\underline{r}') \cdot \underline{\underline{G}}_0(\underline{r}';\underline{r}_0) \; dV' \tag{19}$$

Using equations 10 and 11 as well as the fact that

$$\hat{n}(\underline{r}') \times \underline{E}(\underline{r}') = 0 \quad \underline{r}' \epsilon (S_m - S_1 - S_2) \cup S_p \cup (S_r - S_g) \tag{20}$$

we find that

$$\int_{S_p} \left\{ \hat{n}, \underline{E}_0, \underline{H}_0, \underline{\underline{G}}_0 \right\} dS' = 0 \tag{21}$$

15

$$\int_{S_r} \left\{ \hat{n}, \underline{E}_0, \underline{H}_0, \underline{\underline{G}}_0 \right\} dS' = \int_{S_g} i\omega\epsilon_0 \left[\hat{n}(\underline{r}') \times \underline{E}(\underline{r}') \right] \cdot \underline{\underline{G}}_0(\underline{r}'; \underline{r}_0) \ dS'$$

$$\equiv \underline{S}(\underline{r}_0) \tag{22}$$

$$\int_{S_m} \left\{ \hat{n}_\alpha, \underline{E}_\alpha, \underline{H}_\alpha, \underline{\underline{G}}_\alpha \right\} dS' = i\omega\epsilon_0 \left(\int_{S_1} \left[\hat{n}_\alpha(\underline{r}') \times \underline{E}_\alpha(\underline{r}') \right] \cdot \underline{\underline{G}}_\alpha(\underline{r}'; \underline{r}_\alpha) \ dS' \right.$$

$$\left. + \int_{S_2} \left\{ \hat{n}_\alpha(\underline{r}') \times \underline{E}_\alpha(\underline{r}') \right\} \cdot \underline{\underline{G}}_\alpha(\underline{r}'; \underline{r}_\alpha) \ dS' \right)$$

$$\alpha = 0, I \tag{23}$$

and because $\underline{E}_0$, $\underline{H}_0$, and $\underline{\underline{G}}_0$ satisfy the radiation condition

$$\int_{S_\infty} \left\{ \hat{a}_{r'}, \underline{E}_0, \underline{H}_0, \underline{\underline{G}}_0 \right\} dS' = 0 \tag{24}$$

The remaining quantities to evaluate in equations 16 and 17 are the surface integrals over S_L and S_s. Substituting the equations appropriate for the lossy half space, that is

$$(\nabla' \times \nabla' \times - \omega^2 \mu_0 \epsilon) \underline{H}_L(\underline{r}') = 0 \quad \underline{r}' \epsilon V_L \tag{25}$$

and

$$\nabla' \times \underline{H}_L(\underline{r}') = -i\omega\epsilon \underline{E}_L(\underline{r}') \quad \underline{r}' \epsilon V_L \tag{26}$$

as well as equation 13 into 8 we obtain

16

$$\int_{S_L} \left\{ \underline{H}_L(\underline{r}') \cdot \left[\hat{n}(\underline{r}') \times \left\{ \nabla' \times \underline{\underline{G}}_L(\underline{r}';\underline{r}) \right\} \right] + i\omega\varepsilon \left[\hat{n}(\underline{r}') \times \underline{E}_L(\underline{r}') \right] \underline{\underline{G}}_L(r';r) \right\} dS'$$

$$+ \int_{S_\infty} \left\{ \underline{H}_L(\underline{r}') \cdot \left[\hat{n}(\underline{r}') \times \left\{ \nabla' \times \underline{\underline{G}}_L(\underline{r}';\underline{r}) \right\} \right] + i\omega\varepsilon \left[\hat{n}(r') \times \underline{E}_L(r') \right] \underline{\underline{G}}_L(\underline{r}';\underline{r}) \right\} dS' = 0$$

$$(27)$$

The second integral in equation 27 is zero due to the losses in V_L (or the radiation condition if V_L is lossless). Using the fact that the tangential components of $\underline{E}$ and $\underline{H}$ are continuous across S_L as well the boundary conditions in equation 12a and 12b we see that the integral over S_L in equation 16 is equal to the integral over S_L in equation 27 which in turn we have just shown to equal zero. The integral over S_s will also equal zero and the manner in which this can be seen depends on the physical properties of the subsystem occupying V_s. If it were totally metallic, the boundary conditions on $\underline{E}_I$ and $\underline{\underline{G}}_I$ would make the surface integral vanish in the same manner they did for the integral over S_p. If it were a homogeneous dielectric, then the boundary conditions would cause the surface integral over S_s in the same manner the surface integral over S_L was caused to vanish. If it were some hybrid of dielectric and metal, a combination of the arguments would be used to cause the surface integral to vanish.

We can now write equations 16 and 17 as

$$\underline{H}_0(\underline{r}_0) = \underline{F}(\underline{r}_0) - K_0 \underline{J}_m(\underline{r}') \qquad (28)$$

and

$$\underline{H}_I(\underline{r}_I) = K_I \underline{J}_m(\underline{r}') \qquad (29)$$

17

where

$$\underline{F}(\underline{r}_0) = \underline{I}(\underline{r}_0) + \underline{S}(\underline{r}_0) \tag{30}$$

with $\underline{I}(\underline{r}_0)$ and $\underline{S}(r_0)$ defined by equations 19 and 22 and the operators K_α are defined by

$$K_\alpha \underline{J}_m(\underline{r}') = i\omega\varepsilon_0 \left(\int_{S_1} \underline{J}_m(\underline{r}') \cdot \underline{\underline{G}}_\alpha(\underline{r}', r_\alpha) \ dS' \right.$$

$$\left. + \int_{S_2} \underline{J}_m(r') \cdot \underline{\underline{G}}_\alpha(\underline{r}', \underline{r}_\alpha) \ dS' \right)$$

$$\alpha = 0, I \tag{31}$$

and we have made use of the fact that the tangential components of the electric field are continuous through the apertures so that

$$-\hat{n}_0(\underline{r}') \times \underline{E}_0(\underline{r}') = \hat{n}_I(\underline{r}') \times \underline{E}_I(\underline{r}') = \underline{J}_m(\underline{r}') \qquad \underline{r}' \epsilon S_1 US_2 \tag{32}$$

Now we focus our attention on $\underline{F}(\underline{r}_0)$ appearing in equation 28. The meaning of this quantity is an extremely important aspect of the theory behind portable EMP simulators. It would be a very difficult task to evaluate equations 19, 22, and 30 in order to determine the full significance of $\underline{F}(\underline{r}_0)$. Instead, we will simply utilize certain key features of those equations as well as equations 28 and 31 to determine what $\underline{F}(\underline{r}_0)$ must be if all the required equations were evaluated. First, we note according to equation 19 that $\underline{I}(\underline{r}_0)$ is excited by the rigid (interaction independent) source $\underline{J}(\underline{r}')$ and that according to equation 22, $\underline{S}(\underline{r}_0)$ is excited by the rigidly specified $\hat{n}(\underline{r}') \times \underline{E}(\underline{r}')$ for $\underline{r}' \epsilon S_g$. Next, we note that according to these equations, both $\underline{I}(\underline{r}_0)$ and $\underline{S}(\underline{r}_0)$ are insensitive to the size

of the apertures S_1 and S_2 and in fact they are insensitive to whether or not these apertures are even present. Using these observations in conjunction with equation 31 as the aperture size becomes zero and using the result in equation 28, we see that $\underline{F}(\underline{r}_0)$ equals $\underline{H}_0(\underline{r})$ for the special case where all apertures are sealed (short circuited). Mathematically, we express this evaluation of $\underline{F}(\underline{r}_0)$ as

$$\underline{F}(\underline{r}_0) = \underline{H}_0^{s.c.}(\underline{r}_0) \tag{33}$$

where the superscript is introduced to indicate "short circuit." We note that $\underline{F}(\underline{r}_0)$ is the short circuit magnetic field at some point $\underline{r}_0$ with apertures sealed, but all other aspects of the external environment including the proximity and structure of the radiator, S_r, unchanged.

Substituting equation 33 into equation 28 we obtain

$$\underline{H}_0(\underline{r}_0) = \underline{H}_0^{s.c.}(\underline{r}_0) - K_0 \underline{J}_m(\underline{r}') \tag{34}$$

Next, we define $\hat{n}(\underline{r}) = \hat{n}_I(\underline{r}) = -\hat{n}_0(\underline{r})$ for $\underline{r} \epsilon S_1 U S_2$, use the fact that

$$\hat{n}(\underline{r}) \times \underline{H}_0(\underline{r}) = \hat{n}(\underline{r}) \times \underline{H}_I(\underline{r}) \tag{35}$$

and employ equations 28 and 34 to obtain

$$\lim_{\substack{\underline{r}_0 \to \underline{r} \\ \underline{r}_I \to \underline{r}}} \hat{n}(\underline{r}) \times (K_0 + K_I) \underline{J}_m(\underline{r}') = \underline{J}_{E.I.}(\underline{r}) \tag{36}$$

where we have used the definition

$$\hat{n}(\underline{r}) \times \underline{H}_0^{s.c.}(\underline{r}) \equiv \underline{J}_{E.I.}(\underline{r}) \tag{37}$$

19

and we have the desired result, in that equation 36 is the more detailed representation of equation 1.

Before we can present our theoretical conclusions, we must present our more detailed representation of equation 2. We have, in fact, already a representation of equation 2 for the case where the desired internal electrical quantity is the magnetic field. For that use we might choose the symbol β as H so that $Q_H = \underline{H}$ and $L_\beta = L_H = K_I$. Another example where the structure of L_β changes depending on the choice of Q_β is readily demonstrated by considering the case where the desired internal electrical quantity is the electric field $\underline{E}$ and we denote β as E so that $Q_E = \underline{E}$. For this case equation 2 becomes

$$Q_E = L_E \underline{J}_m(\underline{r}) \tag{38}$$

where

$$L_E = -\frac{1}{i\omega\varepsilon_0}\nabla \times K_I \tag{39}$$

Finally, we will discuss the more important case where the desired internal electrical quantity is a current. For this discussion consider that part of the internal subsystem occupying volume V_s in figure 1 contains a wire and we choose a local cylindrical coordinate system having its axis along the wire and having the local azimuthal vector denoted $\hat{\phi}_w(\ell')$ at the point on the wire where we wish to determine the current. The argument of this unit vector, ℓ', denotes the circumferential position on the wire. With these definitions, the current on the wire is

$$I = \oint d\ell' \hat{\phi}_w(\ell') \cdot \underline{H}_I(\underline{r}_I) \tag{40}$$

20

We see that from equations 29 and 40 that

$$Q_c = L_c J_m(\underline{r}')$$ (41)

where we have denoted $I = Q_c$ and

$$L_c J_m(\underline{r}') \equiv \oint d\ell' \hat{\phi}_w(\ell') \cdot K_I J_m(\underline{r}')$$ (42)

We have now presented equations 1 and 2 in sufficient detail to draw our desired conclusions. We will base our conclusions on equation 4 which contains exactly the physics as do equations 1 and 2. The specific points we wish to make are i) the external interaction current density, $\underline{J}_{E.I.}$, can be excited by either a rigid source, a non-rigid source, or a combination of the two types ii) the transfer operator, T_β^α, depends on the external environment to the system iii) T_β^α depends on the internal environment iv) T_β^α depends on the internal electrical quantity, Q_β, being determined v) T_β^α depends on the rigidity of the source. Equations that specifically illustrate each of these points are identified with the numbered points as follows: i) equations 19, 22, 30, 33, and 37 ii) equations 11 and 12 iii) equation 10 as well as the argument that eliminated the integral over S_s iv) equations 5, 39, and 42 v) equation 11.

The remaining portion of this report will be devoted to the calculation that represents the idealized experiment.

SECTION III

MAGNETIC FIELD INTEGRAL EQUATION FOR A SPHERE

If we impose an orthonormal coordinate system $\hat{s}, \hat{t}$ on a closed surface possessing continuous curvature such that $\hat{s} \times \hat{t} = \hat{n}$, the outward normal to the body, we can write the Magnetic Field Integral Equation (MFIE) as the following system of coupled scalar integral equations

$$\frac{1}{2} J_s(\underline{r}) = -\hat{t}(\underline{r}) \cdot \underline{H}^{inc}(\underline{r}) + \int \Big(A(\underline{r}, \underline{r}') J_s(\underline{r}')$$

$$+ B(\underline{r}, \underline{r}') J_t(\underline{r}') \Big) dS' \qquad (43a)$$

$$\frac{1}{2} J_t(\underline{r}) = \hat{s}(\underline{r}) \cdot \underline{H}^{inc}(\underline{r}) + \int \Big(C(\underline{r}, \underline{r}') J_s(\underline{r}')$$

$$+ D(\underline{r}, \underline{r}') J_t(\underline{r}') \Big) dS' \qquad (43b)$$

where

$$A(\underline{r}, \underline{r}') = -Q(|\underline{r} - \underline{r}'|) \Big[\hat{t}(\underline{r}) \cdot (\underline{r} - \underline{r}') \times \hat{s}(\underline{r}') \Big] \qquad (44a)$$

$$B(\underline{r}, \underline{r}') = -Q(|\underline{r} - \underline{r}'|) \Big[\hat{t}(\underline{r}) \cdot (\underline{r} - \underline{r}') \times \hat{t}(\underline{r}') \Big] \qquad (44b)$$

$$C(\underline{r}, \underline{r}') = Q(|\underline{r} - \underline{r}'|) \Big[\hat{s}(\underline{r}) \cdot (\underline{r} - \underline{r}') \times \hat{s}(\underline{r}') \Big] \qquad (44c)$$

$$D(\underline{r}, \underline{r}') = Q(|\underline{r} - \underline{r}'|) \Big[\hat{s}(\underline{r}) \cdot (\underline{r} - \underline{r}') \times \hat{t}(\underline{r}') \Big] \qquad (44d)$$

$$Q(R) = (ikR - 1) \frac{e^{ikR}}{4\pi R^3} \qquad (45)$$

and $J_s(\underline{r})$, $J_t(\underline{r})$ are defined through

$$\underline{J}(\underline{r}) \equiv J_s(\underline{r}) \hat{s}(\underline{r}) + J_t(\underline{r}) \hat{t}(\underline{r}) \qquad (46)$$

22

For a sphere of radius "a" centered at the origin, $\hat{n}=(\underline{r}/a)$ for all points on the surface. This permits us to greatly simplify the form of equations 44a - 44d even before specifying our actual choice for $\hat{s}$ and $\hat{t}$. Formal manipulation of the triple products in these equations yield

$$A(\underline{r},\underline{r}') = -aQ(\underline{r}-\underline{r}')\left[\hat{s}(\underline{r})\cdot\hat{s}(\underline{r}')-\hat{t}(\underline{r})\cdot\hat{t}(\underline{r}')\right] \quad (47a)$$

$$B(\underline{r},\underline{r}') = -aQ(\underline{r}-\underline{r}')\left[\hat{s}(\underline{r})\cdot\hat{t}(\underline{r}')+\hat{t}(\underline{r})\cdot\hat{s}(\underline{r}')\right] \quad (47b)$$

$$C(\underline{r},\underline{r}') = aQ(\underline{r}-\underline{r}')\left[-\hat{t}(\underline{r})\cdot\hat{s}(\underline{r}')-\hat{s}(\underline{r})\cdot\hat{t}(\underline{r}')\right] \quad (47c)$$

and

$$D(\underline{r},\underline{r}') = aQ(\underline{r}-\underline{r}')\left[-\hat{t}(\underline{r})\cdot\hat{t}(\underline{r}')+\hat{s}(\underline{r})\cdot\hat{s}(\underline{r}')\right] \quad (47d)$$

thus showing that $D(\underline{r},\underline{r}') = -A(\underline{r},\underline{r}')$ and $C(\underline{r},\underline{r}') = B(\underline{r},\underline{r}')$. We also note that $A(\underline{r},\underline{r}') = A(\underline{r}',\underline{r})$ and $B(\underline{r},\underline{r}') = B(\underline{r}',\underline{r})$. This latter symmetry property is of considerable importance for analytic treatments of the MFIE on a sphere, but will be lost in the numerical scheme for solving the equations.

A numerical implementation of equations 43a and 43b even with the simplifications of equations 47a - 47d requires that the sphere be imbedded in some coordinate system. We use a spherical coordinate system, i.e., an arbitrary position on the surface of the sphere has cartesian coordinates

$$\underline{r}(\theta;\phi) = a(\cos\phi\sin\theta,\sin\phi\sin\theta,\cos\theta) \quad (48)$$

23

We may define

$$\hat{t}(\theta,\phi) \equiv -\hat{e}_\theta \equiv \frac{-1}{a} \frac{\partial}{\partial\theta} \underline{r}(\theta,\phi) = (-\cos\phi\cos\theta, -\sin\phi\cos\theta, \sin\theta) \quad (49a)$$

and

$$\hat{s}(\theta,\phi) \equiv \hat{e}_\phi \equiv \frac{1}{a\sin\theta} \frac{\partial}{\partial\phi} \underline{r}(\theta,\phi) = (-\sin\phi, \cos\phi, 0) \quad (49b)$$

obtaining

$$\hat{n}(\theta,\phi) \equiv \hat{s}(\theta,\phi) \times \hat{t}(\theta,\phi) \equiv \frac{1}{a} \underline{r}(\theta,\phi) = (\cos\phi\sin\theta, \sin\phi\sin\theta, \cos\theta)$$
$$(49c)$$

as it should.

Inserting equations 48, 49a and 49b into equations 47a - 47d and recalling that the element of area on the surface of a sphere is $a^2\sin\theta d\theta d\phi$ completes the specification of the MFIE in a spherical coordinate system.

Our procedure for solving the coupled scalar equations of the MFIE is to partition the sphere into zones S_j by an algorithm which has the maximum separation of any two points of any zone tend to zero as the number of zones tends to infinity. We then approximate both J_s and J_t by piecewise constant functions whose discontinuities occur at the zone boundaries. If we pick a representative point from each zone and restrict $\underline{r}$ to this set of points, we obtain, as a matrix approximation to the MFIE,

$$\frac{1}{2} J_s(\underline{r}_i) = -\hat{t}(\underline{r}_i) \cdot \underline{H}^{inc}(\underline{r}_i) + \sum_j J_s(r_i) \int_{S_j} A(\underline{r}_i, \underline{r}') \, dS'$$

$$+ \sum_j J_t(r_i) \int_{S_j} B(\underline{r}_i, \underline{r}') \, dS' \quad (50a)$$

24

$$\frac{1}{2} J_t(\underline{r}_i) = \hat{s}(\underline{r}_i) \cdot \underline{H}^{inc}(\underline{r}_i) + \sum_j J_s(\underline{r}_i) \int_{S_j} C(\underline{r}_i, \underline{r}') \, dS'$$

$$+ \sum_j J_t(\underline{r}_i) \int_{S_j} D(\underline{r}_i, \underline{r}') \, dS' \qquad (50b)$$

This method of solution can be viewed as either a method of moments solution or as a product integration method.

We must, however, consider the nature of the integrands in equations 50a and 50b. One can show that for an arbitrary body with everywhere continuous, non-zero, local curvature A, B, C, and D are singular but behave at worst as $\alpha/|\underline{r}-\underline{r}'|$ as $\underline{r}'$ approaches $\underline{r}$ for some finite α. This will be explicitly shown for the case of a sphere. Since we are dealing with a two-dimensional integral, these integrands are still absolutely integrable, however, these singularities should be treated analytically in order to avoid convergence problems for numerical integration. Our programs for scattering from cylindrical bodies remove this singularity before attempting the numerical integration; experience indicates that such treatment greatly improves the accuracy of both phase calculations and resonant phenomena.

For a sphere, the numerical problem is much simpler. As will be shown by the following analysis, a symmetric integration procedure will permit the singularities to be ignored for sufficiently large zones. By expanding the scalar triple products to second order in $\theta-\theta'$ and $\phi-\phi'$ we will show, as we mentioned earlier, that the above mentioned singularity does exist, but numerical techniques exist which avoid the need to treat the singularity analytically.

We start by expanding $|\underline{r}-\underline{r}'|^2$ in powers of $(\theta-\theta')$ and $(\phi-\phi')$.

$$|\underline{r}-\underline{r}'|^2 = |\underline{r}'|^2 + |\underline{r}|^2 - 2(\underline{r} \cdot \underline{r}') = 2a^2(1-\hat{n}\cdot\hat{n}') \qquad (51)$$

25

which by equation 49c yields

$$|\underline{r}-\underline{r}|^2 = 2a^2\left[1-\sin\theta\sin\theta'(\cos\phi\cos\phi'+\sin\phi\sin\phi')-\cos\theta\cos\theta'\right]$$

$$= a^2\left[\sin^2\theta(\phi-\phi')^2 + (\theta-\theta')^2\right]+o\left[(\theta-\theta')^2 + (\phi-\phi')^2\right] \quad (52)$$

Similarly, from equations 49a, 49b and 47a we get

$$\frac{-A(\underline{r},\underline{r}')}{aQ} = \sin\phi\sin\phi' + \cos\phi\cos\phi'$$

$$-(\cos\phi\cos\phi'\cos\theta\cos\theta'+\sin\phi\sin\phi'\cos\theta\cos\theta'+\sin\theta\sin\theta')$$

$$= \frac{1}{2}\left[(\theta-\theta')^2-\sin^2\theta(\phi-\phi')^2\right]+o\left[(\phi-\phi')^2+(\theta-\theta')^2\right] \quad (53)$$

while equations 49a, 49b and 47b yield

$$\frac{-B(\underline{r},\underline{r}')}{aQ} = -a(\phi-\phi')(\theta-\theta')\sin\theta +o\left[(\phi-\phi')^2+(\theta-\theta')^2\right] \quad (54)$$

The above analysis has shown that neither A nor B behaves any worse than $\alpha/|\underline{r}-\underline{r}'|$ for some finite α, yet, except at the poles (B is non-singular if $\theta = 0$) there exists directions of approach such that both A and B vary as $1/|\underline{r}-\underline{r}'|$ as $\underline{r}'$ approaches $\underline{r}$. In addition, we have shown that except at $\theta=0$ and $\theta=\pi$ B is antisymmetric in $(\theta-\theta')$ and $(\phi-\phi')$ and A is antisymmetric in $(\theta-\theta') \pm (\phi-\phi')\sin\theta$. Thus if our integration scheme is symmetric in $(\theta-\theta')$ and $(\phi-\phi') \pm (\phi-\phi')\sin\theta$ the singular part effectively vanishes for self term interactions, i.e., when i=j for equations 50a and 50b. However, neighboring zone interactions do not necessarily have this antisymmetry property. If wavelength considerations force the zones to be small the singularities should be treated analytically.

26

Our experience has shown that the zoning criteria for accurate solution of the MFIE can be split into wavelength and geometry considerations. As a general rule, between six and ten zones per wavelength are needed to fulfill the wavelength requirements. For this special case we found that we could employ even fewer zones for wavelength. For low frequency, however, geometric considerations dominate the zoning criteria. The adequacy of the geometric requirements can be ascertained by examining the results for magnetostatic excitation. Studying both types of zone requirements, we found that the nearest neighbor zones are far enough removed to permit simple integration schemes for evaluating the integrals of equations 50a and 50b.

SECTION IV

PRESENTATION OF SPHERE CALCULATIONS

The coordinate system, incident field description, and zone numbering scheme for this calculation are depicted in figure 2. The boundaries for each zone are determined by allowing 45° increments in θ and ϕ. In figures 3 through 11 we present the current density induced by the depicted incident field as well as by selected local excitation. What is meant by the local excitation is that a numbered patch is either considered to be illuminated by the depicted incident field or is considered to receive no incident illumination. A discussion of the relevance of this type of local illumination will be deferred to the next section.

The labeling of the tangential components of the induced current density is as follows

$$J_s = J_\phi \tag{55}$$

$$J_t = -J_\theta \tag{56}$$

and the quantities plotted are the magnitudes of these components of current density normalized to the magnitude of the incident magnetic field, H_0. The code verification data presented in these figures comes from two sources. For ka=0, the magnitude of the magnetostatic solution given by

$$J_s = -(3/2) H_0 \cos\phi \cos\theta \tag{57}$$
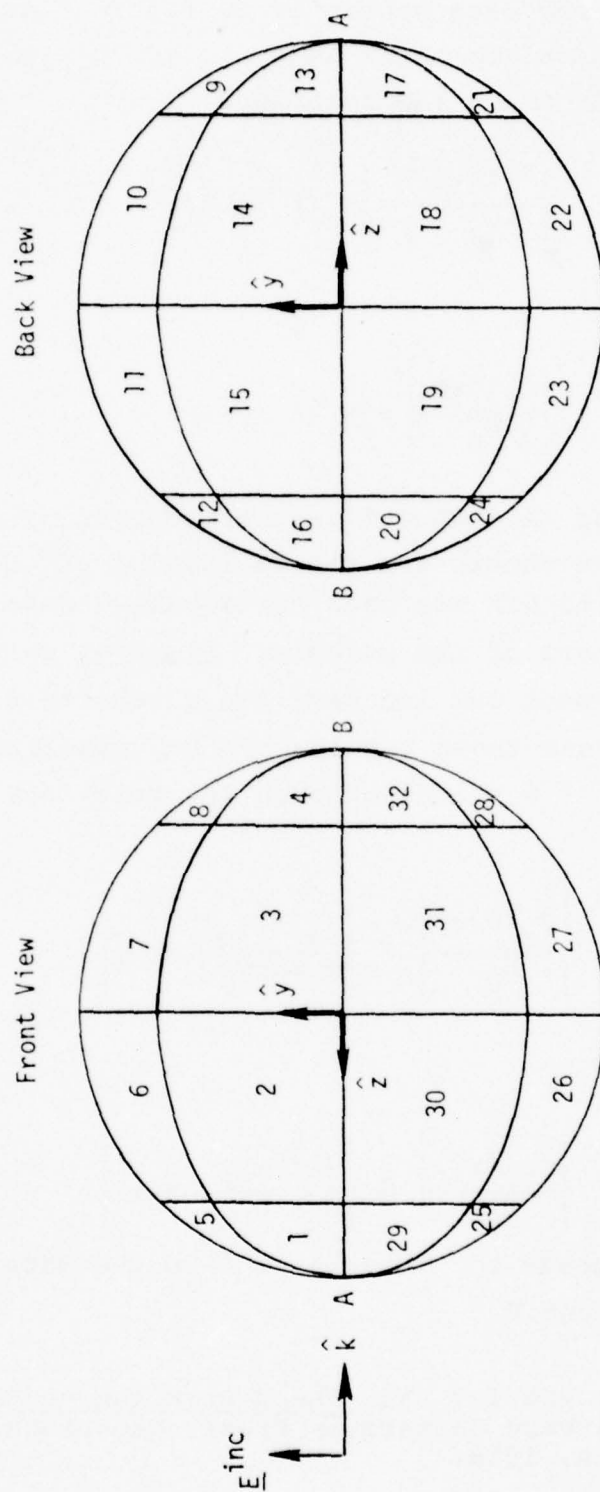
and

$$J_t = -(3/2) H_0 \sin\phi \tag{58}$$

28

Figure 2. Coordinate System and Zone Numbering Scheme for the Sphere Calculations

is used to obtain the code verification data. For k =1.1, 1.7,
2.3, 2.9 we use the data presented in figure 66a of reference 1.
Specifically, we relate their data, K_θ and K_z, to the code
verification data using the relations

$$\left| \frac{J_s(\theta,\phi)}{H_0} \right| = \left| K_z(\Psi_1)\cos\phi \right| \tag{59}$$

and

$$\left| \frac{J_t(\theta,\phi)}{H_0} \right| = \left| K_\theta(\theta_1)\sin\phi \right| \tag{60}$$

as well as making the identification $\Psi_1 = \theta_1 = \theta$. The values of
θ and ϕ which are chosen for the evaluation of equations
57, 58, 59, and 60 for the code verification data correspond to
the angular centers of the patches. Finally, we note that
we need only present our incident field results for zones
1 through 8 because those results can be translated to the
remaining range of ϕ values through the relations

$$\left| \frac{J_s(\theta,\phi)}{H_0} \right| = \left| \frac{J_s(\theta,\phi_p)}{H_0\cos\phi_p}\cos\phi \right| \tag{61}$$

and

$$\left| \frac{J_t(\theta,\phi)}{H_0} \right| = \left| \frac{J_t(\theta,\phi_p)}{H_0\sin\phi_p}\sin\phi \right| \tag{62}$$

where ϕ_p corresponds to a value of ϕ in the data presented
for zones 1 through 8.

---

1. King, R.W.P. and T.T. Wu, <u>The Scattering and Diffraction
   of Waves</u>, Harvard University Press, Cambridge,
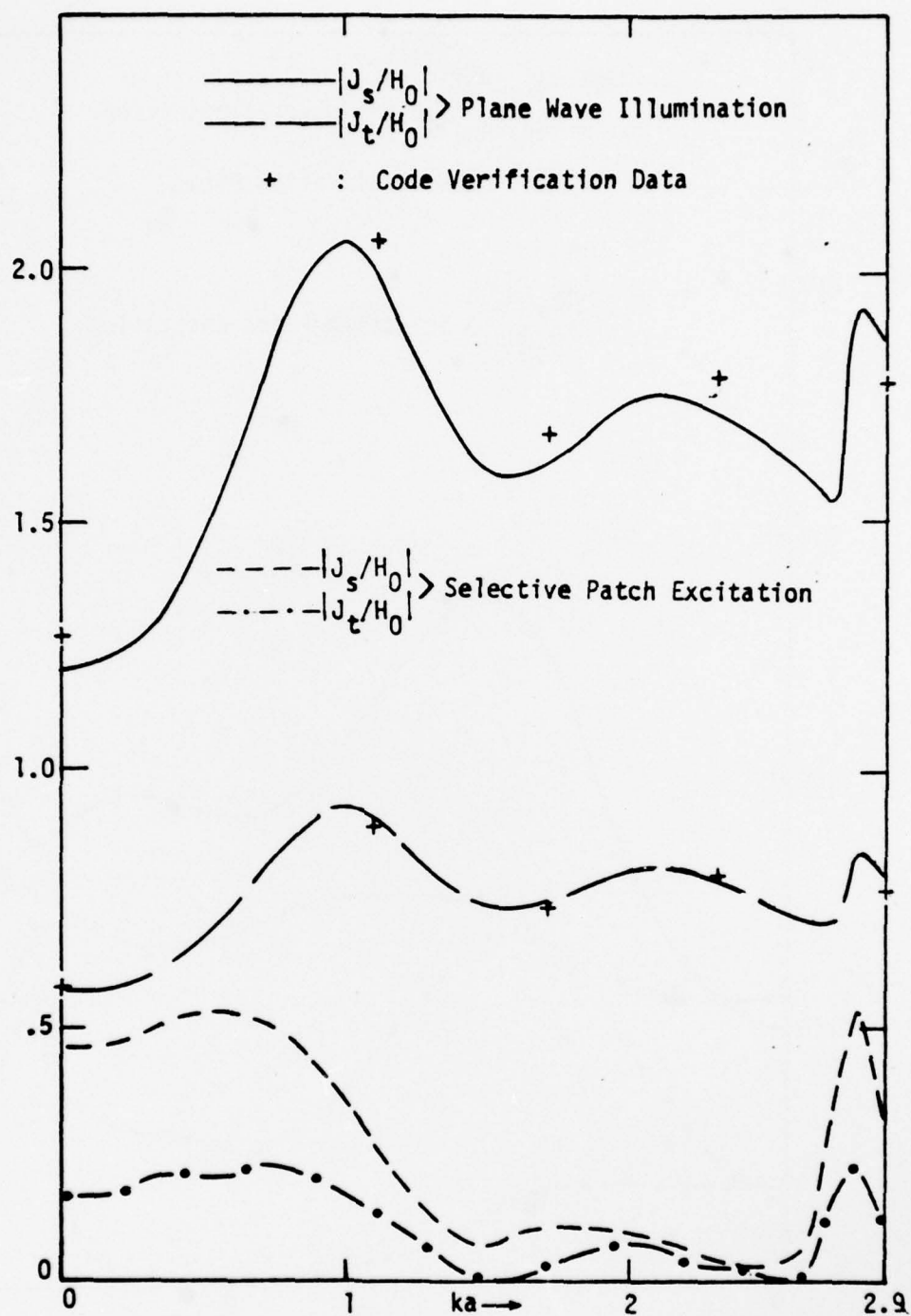   Massachusetts, 1959.

Figure 3. Normalized Current Densities on Patch 1.
Selective Patch Excitation is Achieved by
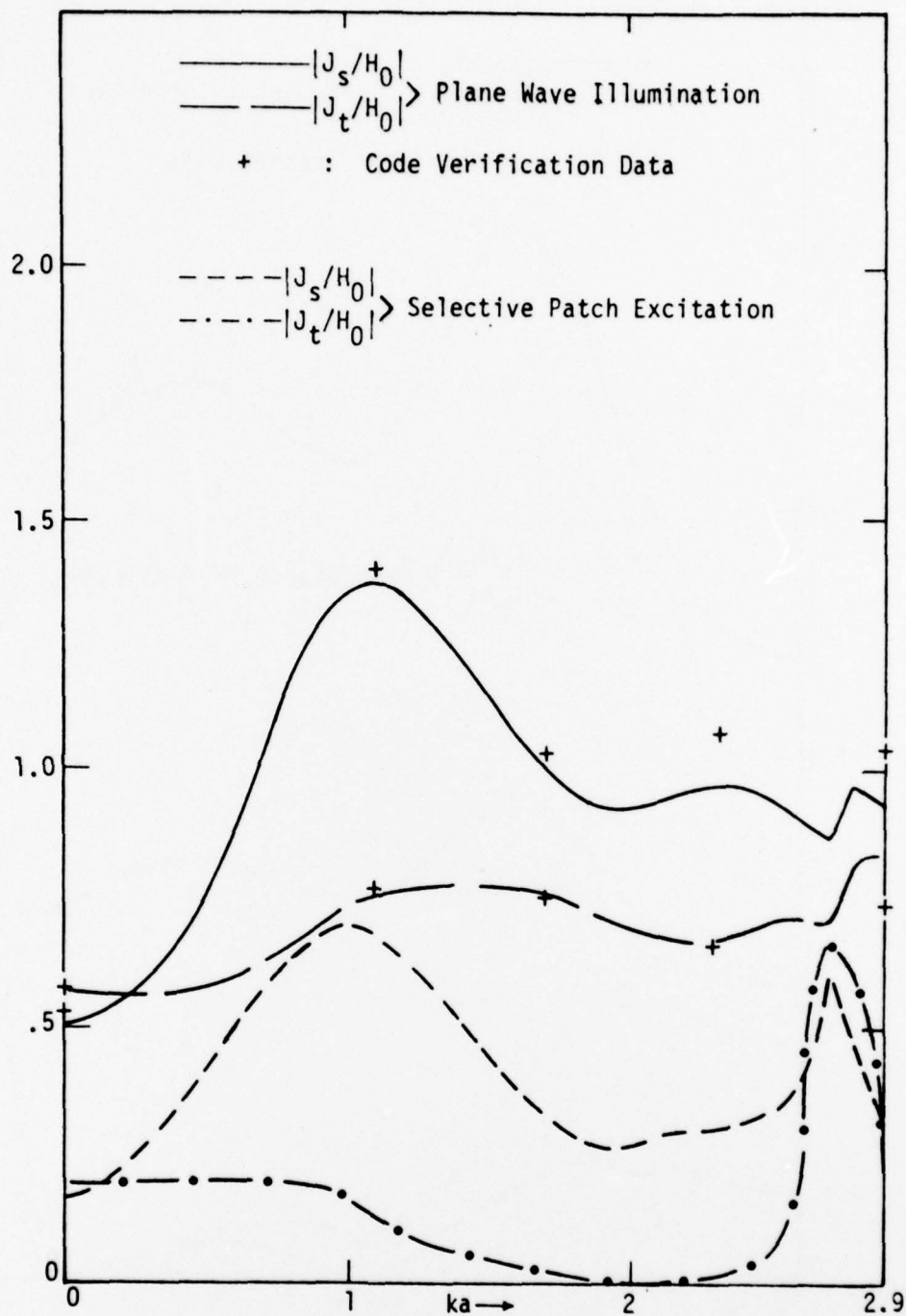Exciting all Patches but No. 1.

31

Figure 4. Normalized Current Densities on Patch 2.
Selective Patch Excitation is Obtained by
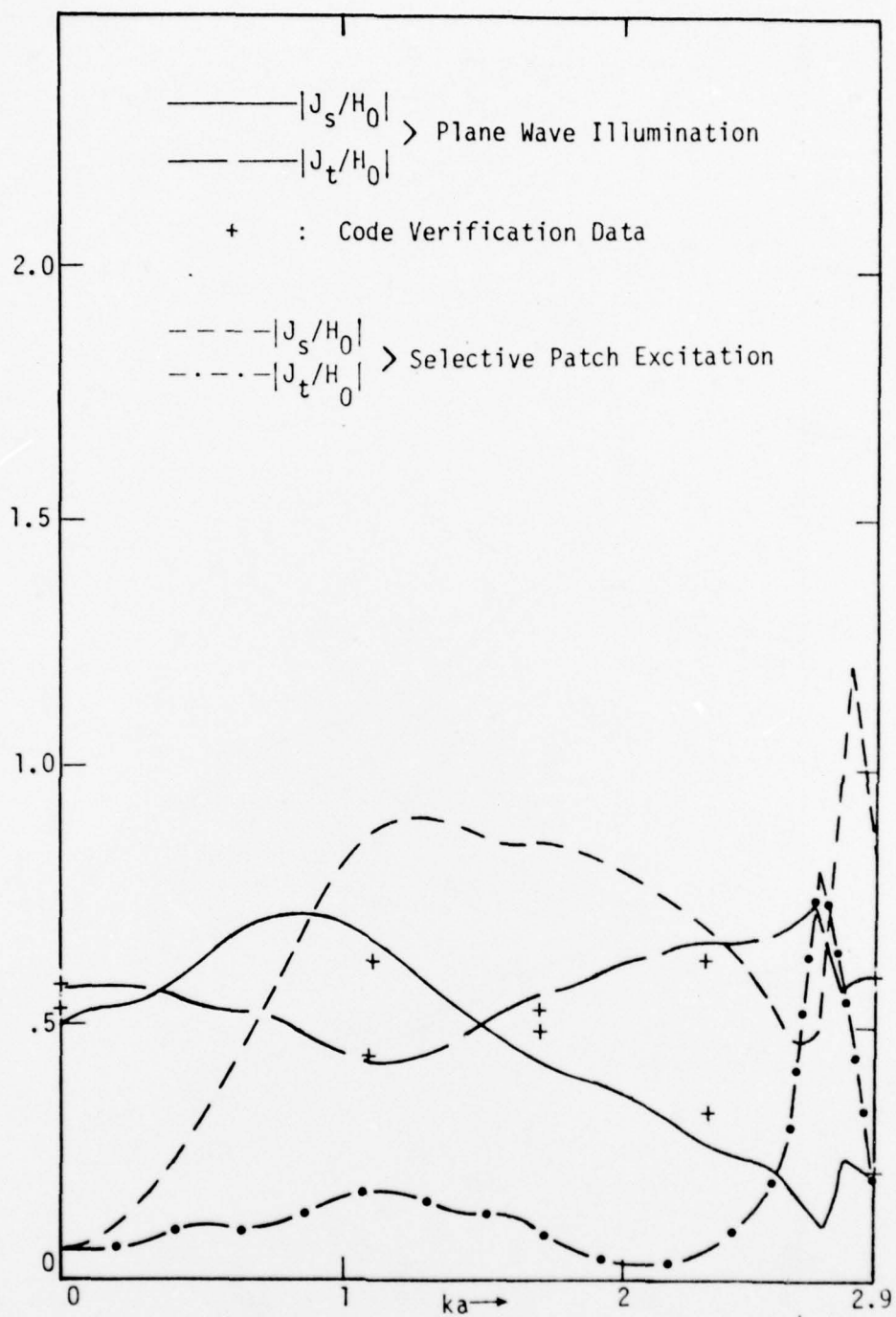Exciting all Patches but No. 2.

32

Figure 5. Normalized Current Densities on Patch 3.
Selective Patch Excitation is Obtained by
Exciting all Patches but
Nos. 2, 3, 14, 15, 18, 19, 30, 31.

Figure 6. Normalized Current Densities on Patch 4.
Selective Patch Excitation is Obtained by
Exciting all Patches but
Nos. 2, 3, 14, 15, 18, 19, 30, 31.

34

Figure 7. Normalized Current Densities on Patch 5.
Selective Patch Excitation is Obtained by
Exciting all Patches but No. 1.

35

Figure 8. Normalized Current Densities on Patch 6.
Selective Patch Excitation is Obtained by
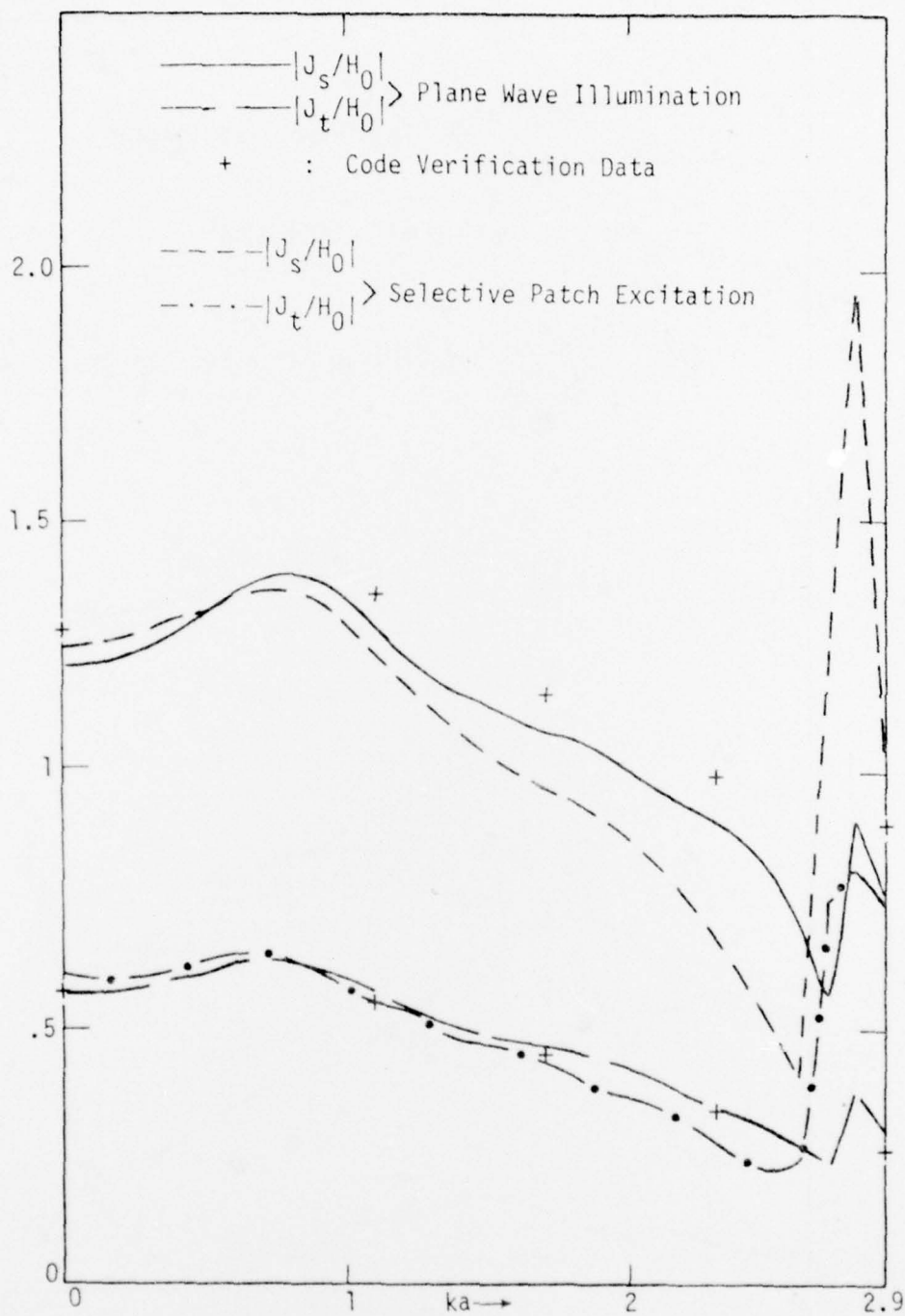Exciting all Patches but No. 2.

Figure 9. Normalized Current Densities on Patch 7.
Selective Patch Excitation is Obtained by
Exciting all Patches but
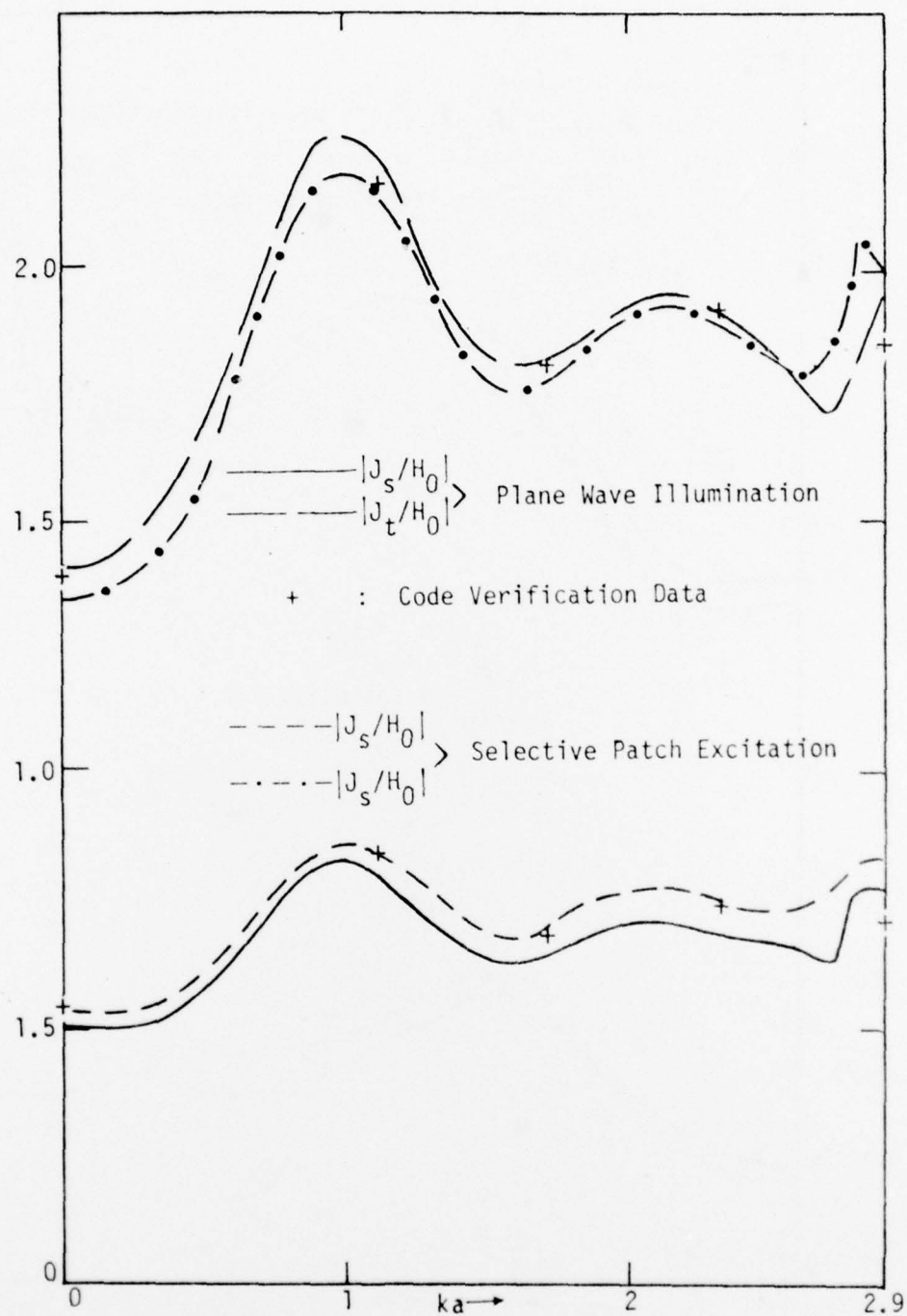Nos. 2, 3, 14, 15, 18, 19, 30, 31.

37

Figure 10. Normalized Current Densities on Patch 8.
Selective Patch Excitation is Obtained by
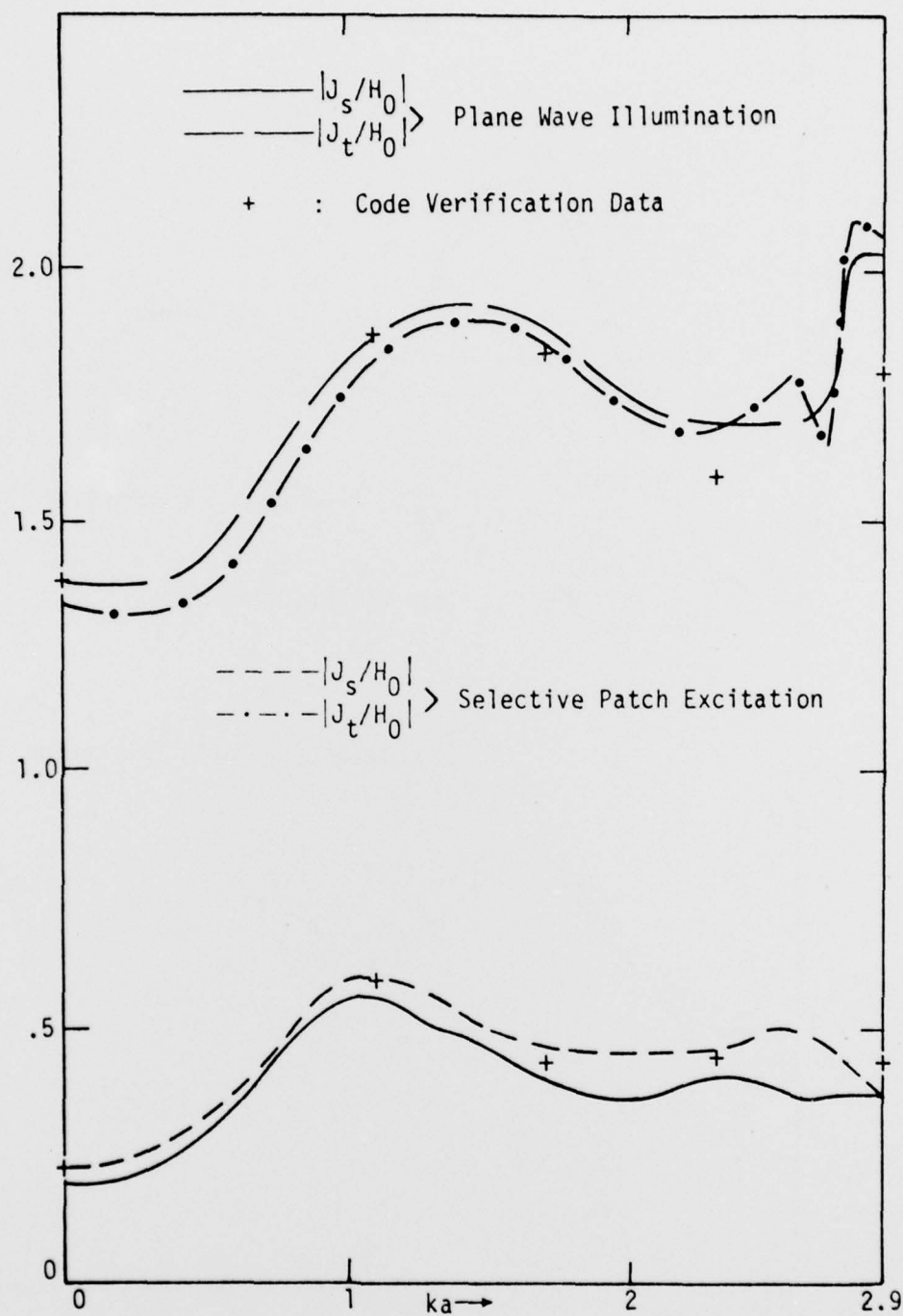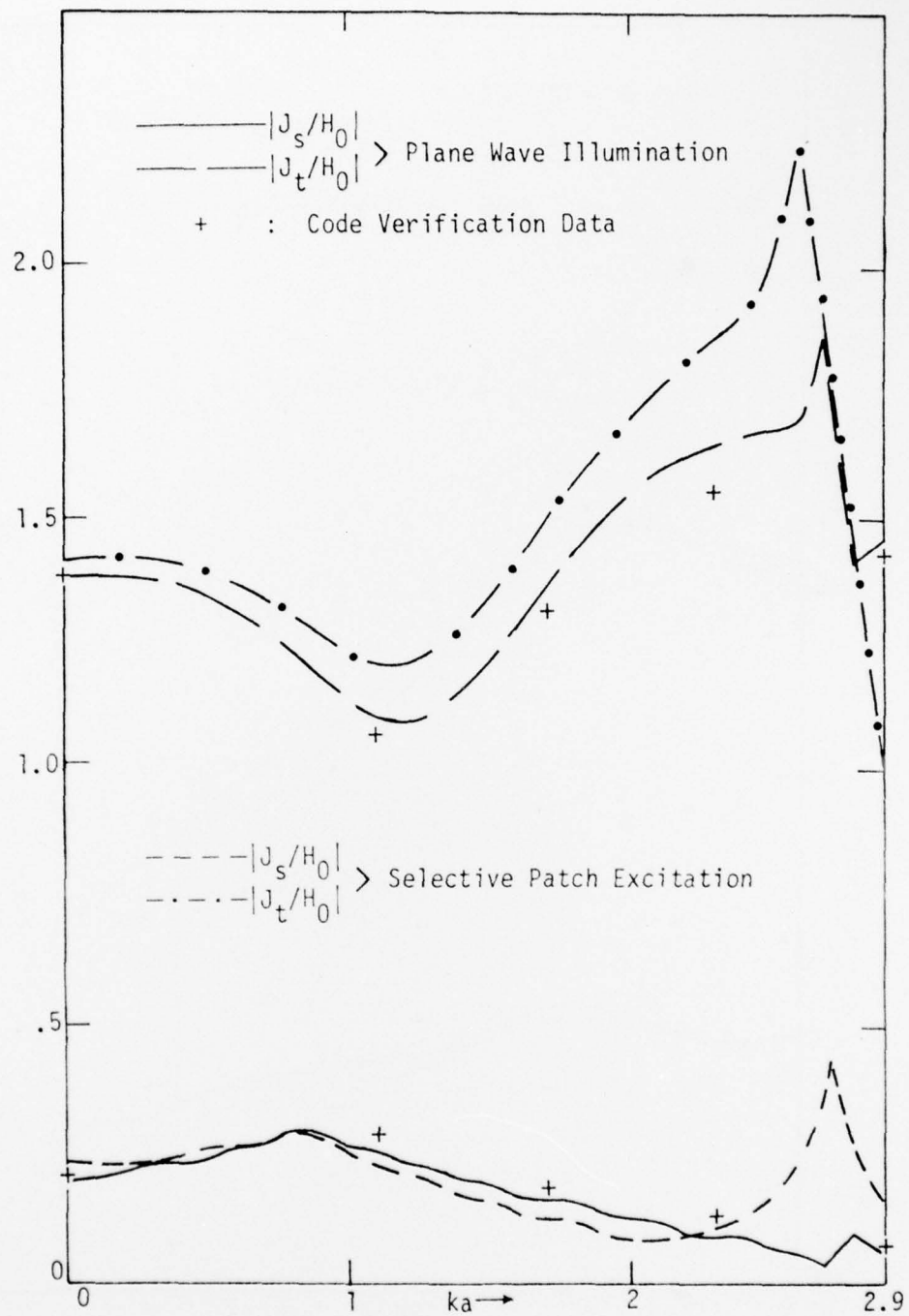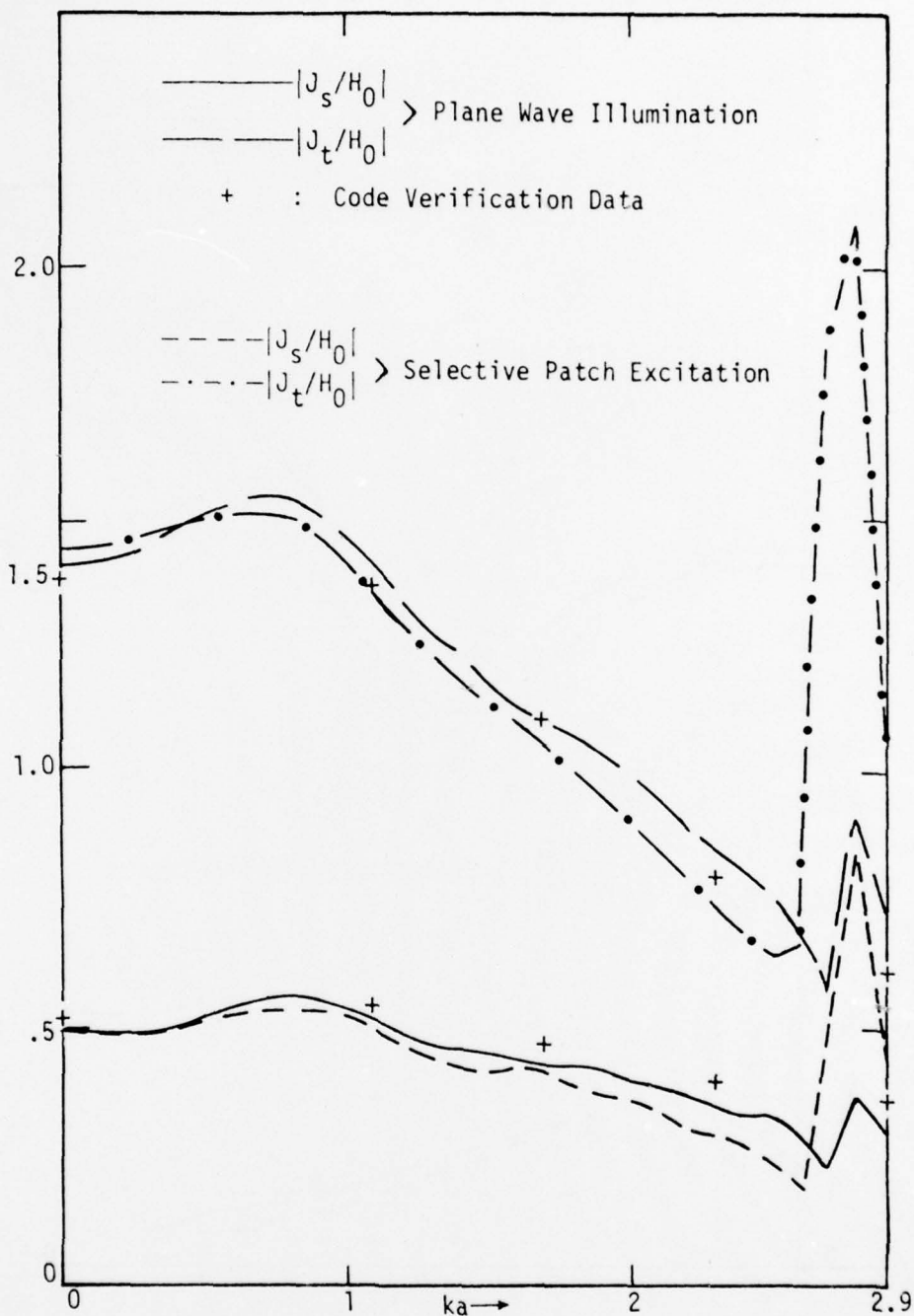Exciting all Patches but
Nos. 2, 3, 14, 15, 18, 19, 30, 31.

38

SECTION V

INTERPRETATION OF SPHERE CALCULATIONS

The basis for our choice of the illumination scheme that
was used to obtain our data is as follows: i) the objective
of each portable simulator was determined only by the incident
field ii) it was easy to numerically implement iii) it bore a
relation to an identifiable class of real sources iv) it had
to succeed as more sources where included. The choice of where
to place the sources is related to the source rigidity issue.
This is readily seen by interpreting the results presented in
figures 3 and 4. In each of these figures, 31 of the 32
patches were illuminated in exactly the same manner that they
would be by the incident plane wave. The only patch that wasn't
excited is the patch on which we present the data and we see
that the induced current density is a very poor approximation
to the desired current density which was induced by the inci-
dent plane wave. This implies that if the non-illuminated
patch corresponds to the shorted POE location, we can obtain
good excitation of that POE only by having a source, of the
type considered in this report, in close proximity.

This result enhances the importance of source rigidity
effects. This is the case because a qualitative examination
of the equations that raised the issue of source rigidity indi-
cates that the nonrigidity effect becomes increasingly impor-
tant as the source location approaches the POE. Determining
the quantitative effect of source rigidity appears to be an
experimental problem. Figures 7 and 8 show that patches adja-
cent to the nonexcited patch can be excited in the desired
manner for the described 31 out of the 32 patch illumination.
This result again, is only meaningful if source rigidity is
not found to be a limiting consideration.

The remaining data appearing in figures 5, 6, 9, and 10 correspond to an illumination scheme in which only 24 of the 32 patches are illuminated. The basis for choosing not to illuminate the eight patches is that they correspond to the smallest values of $\hat{n} \times \underline{H}^{inc}$. For this more sparce illumination scheme we again see that we obtain good results at a patch that is excited and poor results at a patch that is not excited.

Another conclusion worth noting from all the data presented in figures 3 through 10 is that the plane wave illumination results agree reasonably well with the code verification data for ka as large as 2.3. In many cases the agreement is still reasonable for ka=2.9. These results indicate that it is possible to give up a certain measure of accuracy and have fewer zones per wavelength than previously thought. For the data presented, the ratio of the wavelength λ to a zone dimension D is given by $\lambda/D=8/ka$ which is 3.5 if we accepted results only up to ka=2.3 and is 2.8 if we accept the results up to ka=2.9. In either case we see that it is possible to obtain acceptable results with fewer zones than has in general been previously thought. This can impact a scheme for determining a configuration of local sources. The fact that sparce illumination gave good results also provides a rationale for employing fewer sources. Both of these results can assist the choice of a configuration to be employed in an experiment.

At this point, it should be noted that no part of our explicit sphere calculation can be used to infer any experimental information for very early times since our calculation was not appropriate for high frequencies. Another limitation of our calculation should be pointed out. The sphere does not have a sharp resonance and this could contribute to the fact that the patch containing the POE required direct excitation in order for good results to be obtained. For structures having more pronounced resonances, it is possible that near resonance

a given POE can be excited without having the source in as close proximity as indicated by our sphere results. Having elaborated on the limitations of our sphere calculations we would like to emphasize that the general theory presented in this work is valid for all frequencies and consequently all time.

We now address the essential aspects required by our analysis for each local source. In the absence of any other objects and sources, their radiated fields should rapidly decay away from their patch location and at the same time their radiated fields should vary slowly over their own patch location. The simplest source that possesses locality to some extent, is a half-loop placed above the patch. A simple calculation shows that the fields decay rapidly for distances larger than the radius of the loop. Despite its local character which, to a certain degree, satisfies one of our conditions for an allowable source, there are difficulties with the half-loop that we will briefly discuss: i) the field due to a half-loop is slowly varying over a region surrounding the center of the loop but the maximum linear dimension of this region is significantly smaller than the radius of the loop. To remedy this we may either consider a half-loop much larger than the patch or a "solenoid" consisting of many parallel half-loops with its dimensions not significantly larger than the dimensions of the patch. In the case of a large half-loop the incident field will now vary rapidly over other patches, and we have not assessed the effect of this behavior in our calculations. However, the numerical solution is only a convenience for studying selective patch excitation and its inapplicability does not invalidate the potential use of the half-loop as a portable simulator. ii) The "solenoid" is an improvement with regard to the condition of slow variation but it, as well as the large half-loop, may interact with the sphere substantially and this could significantly alter the transfer operator

41

as explained earlier in connection to non-rigidity of sources. Despite all the described limitations, both the "solenoid" and the half-loop have sufficiently desirable features to be included in an experimental program.

Finally, we discuss the Singularity Expansion Method (SEM) as it relates to alternate simulation. We do this because it offers a hope of determining the global capabilities of a configuration of portable sources. We will now interpret our results as related to SEM. An SEM external interaction solution has the form

$$\underline{J}(\underline{r},\gamma) = \sum \eta_\alpha(\gamma) \frac{1}{\gamma-\gamma_\alpha} \underline{\nu}_\alpha(\underline{r})$$

The natural modes $\underline{\nu}_\alpha$ and natural frequencies $\gamma_\alpha c$ are intrinsic properties of the metallic body. The coupling coefficients η_α depend on both the coupling vectors (also an intrinsic property of the body) and the incident field. Thus, once the natural modes, the coupling vectors, and the natural frequencies are known, the responses to various excitations in the SEM prescription are obtained by determining the corresponding coupling coefficients.

Admittedly there is no known recipe for obtaining the coupling coefficients, in general, but at least we know that for the sphere and plane wave illumination the correct coupling coefficients are class 1 given by

$$\eta_{nn'm\sigma p}(\gamma) = e^{(\gamma_{nn'}-\gamma)ct_0} \left[\frac{\left| \underline{\tilde{J}}_{nm\sigma}, \underline{J}_p^{inc} \right|}{N_{nm\sigma}\left[d\lambda_n/d\gamma\right]} \right]_{\gamma=\gamma_{nn'}} \qquad (63)$$

where

$$\left\{ \tilde{\underline{J}}_{nm\sigma}, \underline{J}_p^{inc} \right\} = \int_S \tilde{\underline{J}}_{nm\sigma} \cdot \hat{n} \times \underline{J}_p^{inc} \ dS$$

$$N_{nm\sigma} = \int \tilde{\underline{J}}_{nm\sigma} \cdot \hat{n} \times \underline{J}_{nm\sigma} \ dS$$

$\gamma_{nn'}$ are the pole locations ($\gamma_{nn'} c$ = natural frequencies), t_0 is the instant at which the incident wavefront hits the sphere, $\underline{J}_p^{inc} = \hat{n} \times \underline{H}_p^{inc}$ and p stands for polarization, λ_n are the eigenvalues of the Magnetic Field Integral Operator L, and $\tilde{J}_{nm\sigma}$ are eigenfunctions of L corresponding to eigenvalue $1-\lambda_n$.

If we were to compare responses to selective patch excitation and plane wave illumination, we could assume that the coupling coefficients for patch excitation are also given by equation 1 and proceed to calculate them. The comparison of the coupling coefficients for the two excitations would allow us then to ascertain how well selective patch excitation simulates plane wave illumination. At this point, however, caution should be exercised. To clarify the point we are trying to emphasize, consider the case whereby we excite all patches on the sphere but one, in the manner that was explained. The MFIE solution shows that the total current induced on the sphere is everywhere approximately equal to the current for plane wave illumination except at the center of the patch that was not excited. However, if we were to use SEM for the comparison of the two types of excitation, the coupling coefficients for the first few modes would be approximately equal and this result might lead one to the false conclusion that the simulation was adequate. Notice, however, that our

43

patch zoning results provide no information as to any early-time SEM results and/or conclusions.

DISTRIBUTION LIST

No. Copies

DEPARTMENT OF DEFENSE

12	Defense Documentation Center ATTN: DD

DEPARTMENT OF THE AIR FORCE

2	Air Force Weapons Laboratory ATTN: SUL
1	Air Force Weapons Laboratory ATTN: HO, Dr. Minge
1	Air Force Weapons Laboratory ATTN: NT, Dr. Payton
2	Air Force Weapons Laboratory ATTN: ELTE, Dr. Baum
1	Air Force Weapons Laboratory ATTN: NT, J. Darrah
1	Air Force Weapons Laboratory ATTN: ELT, Dr. Castillo
1	Air Force Weapons Laboratory ATTN: ELTI, Dr. Chen
5	Air Force Weapons Laboratory ATTN: ELTI, Capt Hudson
1	Air Force Weapons Laboratory ATTN: ELTI, Mr. Prather
1	Air Force Weapons Laboratory ATTN: DYC, Dr. Singaraju
1	Air Force Weapons Laboratory ATTN: ELAT, Technical File
1	Air Force Systems Command ATTN: DLWM
1	Air University Library ATTN: LDE
1	PO's Official Record Copy

45/46